



N-Heterocyclic based new nickel–bis(dithiolene) complexes: Synthesis, characterization and properties

Ravada Kishore, Samar K. Das*

School of Chemistry, University of Hyderabad, Hyderabad 500 046, India

ARTICLE INFO

Article history:

Received 9 August 2012

Accepted 27 November 2012

Available online 7 December 2012

Keywords:

Ni–dithiolene complexes

Electronic structures

Electrochemical studies

Solvatochromism

ABSTRACT

Five new nickel–bis(dithiolene) complexes $(\text{PPh}_4)_2[\text{Ni}^{\text{II}}(\text{C}_8\text{H}_2\text{N}_2\text{S}_2\text{R}_2)_2]$ ($\text{R} =$ pyridin-2-yl (**1**), pyridin-3-yl (**2**), thiophen-2-yl (**3**), furan-2-yl (**4**)) and $(\text{PPh}_4)_2[\text{Ni}^{\text{III}}(\text{C}_8\text{H}_2\text{N}_2\text{S}_2\text{R}_2)_2]$ ($\text{R} =$ naphthalen-2-yl (**5**)), have been prepared by the treatment of *N*-heterocyclic based dithiolene ligands with sodium metal in dry methanol followed by the addition of nickel chloride salt. All these dithiolene ligands and metal coordination complexes are characterized by LC–MS-, ^1H NMR- and HRMS-, IR-, UV–Vis–NIR-spectroscopy, routine elemental analysis and cyclic voltammetry. Compounds **2** and **3** are structurally characterized by single crystal X-ray crystallography. Complex **2** crystallizes in monoclinic space group $P2(1)/c$, whereas complex **3** crystallizes in triclinic space group $P\bar{1}$. Both these complexes (**2** and **3**) exhibit two-dimensional supramolecular networks through C–H...N hydrogen bonding interactions in their crystal structures. Nickel(II) compounds **1–4** exhibit a oxidative response in the range of $E_{1/2} = +0.17$ to $+0.21$ V versus Ag/AgCl, whereas, nickel(III) complex **5** shows both oxidative and reductive responses. Compounds **1–4** show electronic absorptions in the region of 630–650 nm, while compound **5** exhibits absorption band at 890 nm. The positions of the absorption maxima in the electronic absorption spectra of compounds **1** and **2** depend on the solvent polarity, whereas absorption bands of complexes **3–5** are not influenced by the solvent polarity.

© 2012 Elsevier Ltd. All rights reserved.

1. Introduction

Metal coordination complexes of dithiolene (1,2-enedithiolate) ligands exhibit significant and diverse properties [1–6]. Among these, nickel based complexes, for example, $[\text{Ni}(\text{S}_2\text{C}_2\text{R}_2)_2]^{n-}$ ($n = 0–2$) attract considerable attention because of their multiple accessible redox states [7]. The redox activity of the dithiolene ligands can be explained by the existence of canonical forms (Scheme 1) [8], because of which, metal can exist in variable oxidation states (+4 to 0). This ambiguity is a classic example of non-innocent behavior [9] of dithiolene ligands. Nickel–dithiolene complexes exhibit interesting properties, such as, metallicity [10], optical nonlinearity [11] and reactivity with olefins leading to olefin purification [12], molecular magnetism [13], and strong absorbance in the near-infrared region, which is important for Q-switching laser applications [14]. Square planar dithiolene coordination complexes are generally characterized by high extent of electron delocalization within the chelate ring involving the metal ion that appreciably contributes to the low energy electronic transition between the HOMO and the LUMO. This extensive delocalization is responsible for metal dithiolene complexes to show an absorption band in its near-infrared (NIR) region [15].

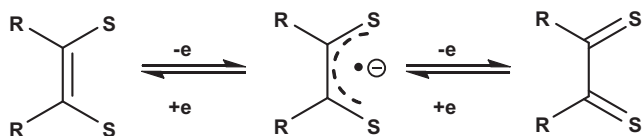
* Corresponding author. Tel.: +91 40 2301 1007; fax: +91 40 2301 2460.
E-mail address: skdsc@uohyd.ernet.in (S.K. Das).

Scheme 2, for example, demonstrates two nickel dithiolene complexes, in which cyano group substituted nickel complex exhibits absorption band at 863 nm and the phenyl substituted metal complex reveals electronic absorption band at 935 nm. This indicates that substituent on dithiolene moiety can influence in the shift of position of electronic absorption band of charge transfer transition, meaning thereby, electron-donating/electron-withdrawing substituents play an important role in the delocalization of the chelate ring in metal–bis(dithiolene) complexes [16–21]. These facts prompted us to design and synthesize new type of *N*-hetero substituent-based (pyridin-2-yl, pyridin-3-yl, thiophen-2-yl, furan-2-yl and naphthalen-2-yl) dithiolene ligands and to synthesize corresponding metal bis(dithiolene) complexes $(\text{PPh}_4)_2[\text{Ni}^{\text{II}}(\text{C}_8\text{H}_2\text{N}_2\text{S}_2\text{R}_2)_2]$ ($\text{R} =$ pyridin-2-yl (**1**), pyridin-3-yl (**2**), thiophen-2-yl (**3**), furan-2-yl (**4**)) and $(\text{PPh}_4)_2[\text{Ni}^{\text{III}}(\text{C}_8\text{H}_2\text{N}_2\text{S}_2\text{R}_2)_2]$ ($\text{R} =$ naphthalen-2-yl (**5**)), which enable us to compare the substituent effect on the redox potentials of the title complexes.

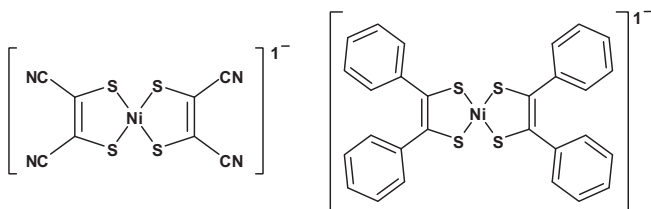
2. Experimental

2.1. Materials and physical methods

All the reagents for synthesis were commercially available and used as received. 4,5-bis-thiocyanato-benzene-1,2-diamine, 5,6-diaminobenzene-1,3-dithiole-2-thione, 1,2-di(pyridin-3-yl)ethane-



Scheme 1. Canonical forms of a dithiolene ligand.



Scheme 2. Nickel dithiolene complexes.

1,2-dione and 1,2-di(naphthalen-2-yl)ethane-1,2-dione were prepared according to literature procedures [22–25]. Solvents were dried by standard procedures. Micro-analytical (C, H, N) data were obtained with a FLASH EA 1112 Series CHNS Analyzer. Infrared spectra were recorded as KBr pellets on a JASCO-5300 FT-IR spectrophotometer at 298 K. Electronic absorption spectra of all compounds were recorded on a Shimadzu UV-Vis-NIR spectrophotometer. NMR spectra were recorded on Bruker 400 and 500 MHz spectrometer. The chemical shifts (δ) are reported in ppm. A Cypress model CS-1090/CS-1087 electro analytical system was used for cyclic voltammetric experiments. The electrochemical experiments were measured in dimethylsulfoxide containing $[\text{Bu}_4\text{N}][\text{ClO}_4]$ (TBAP) as a supporting electrolyte, using a conventional cell consisting of two platinum wires as working and counter electrodes, and a Ag/AgCl electrode as a reference. Under identical condition, Fc^+/Fc couple was observed at 0.53 V. The potentials reported here are uncorrected for junction contributions. The electron paramagnetic resonance (EPR) spectra were recorded on a (JEOL) JESFA200 EPR spectrometer, and the solution state EPR spectra were recorded on a Bruker-ER073 instrument equipped with an EMX microX source for X band measurement using XENON 1.1b.60 software provided by the manufacturer.

2.1.1. General synthetic route for the preparation of the compounds (a–e)

A mixture of solution containing 5,6-diaminobenzo[*d*][1,3]-dithiole-2-thione (1 mmol), corresponding 1,2-diketone (1 mmol), and iodine (10 mol%) in CH_3CN (10.0 mL) was stirred at room temperature for 2 h as shown in scheme 3. The resulting yellow colored precipitate was separated by filtration, washed with little CH_3CN and dried in an open air. The characterization data of these compounds are described in the section of Supplementary data.

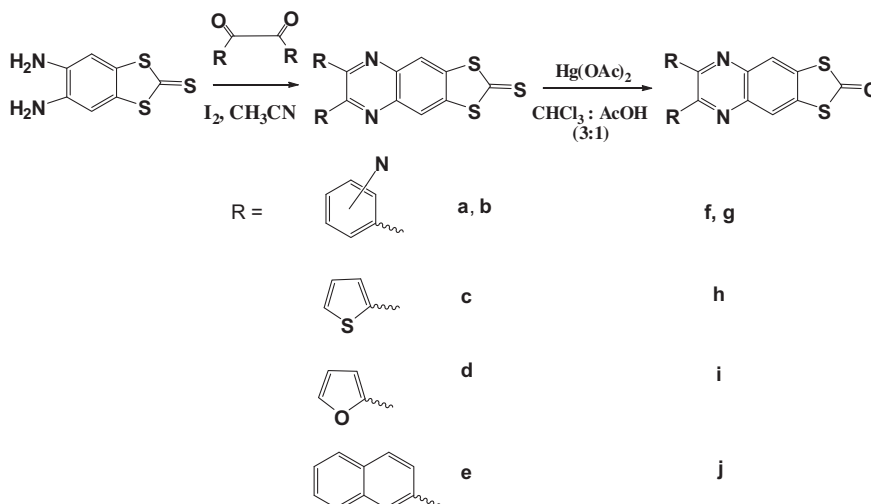
2.1.2. General synthetic route for the preparation of the compounds (f–j)

Following a literature procedure [26], to a chloroform–acetic acid (3:1) solution of each of a–e (1 mmol), $\text{Hg}(\text{OAc})_2$ (3 mmol) was added and it was stirred for 12 h at room temperature under nitrogen atmosphere (Scheme 3). The resulting precipitate was filtered off by using Celite and washed with chloroform. The filtrate was neutralized with NaHCO_3 solution, and extracted with dichloromethane solvent and dried over Na_2SO_4 . The solvent was removed by rotary evaporator which produces pale yellow colored compound as product. The characterization data for f–j are described below:

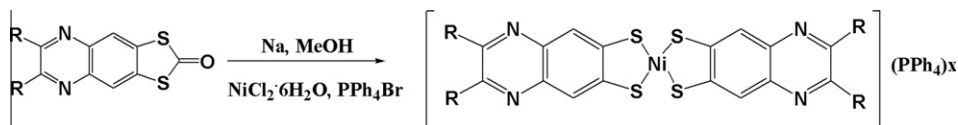
2.1.2.1. 6,7-Di-pyridin-2-yl-1,3-dithia-5,8-diaza-cyclopenta[*b*]naphthalen-2-one (f). (Yield: 92%, 0.344 g). ^1H NMR (400 MHz, δ ppm) ($\text{DMSO}-d_6$): 7.40–7.43 (m, 2H), 8.01–8.06 (m, 4H), 8.30 (s, 2H), 8.75 (s, 2H). LC–MS (ESI): m/z : 375 $[\text{M}+\text{H}]^+$. Anal. Calc. for $\text{C}_{19}\text{H}_{10}\text{N}_4\text{OS}_2$: C, 60.95; H, 2.69; N, 14.96. Found: C, 60.85; H, 2.75; N, 14.69%.

2.1.2.2. 6,7-Di-pyridin-3-yl-1,3-dithia-5,8-diaza-cyclopenta[*b*]naphthalen-2-one (g). (Yield: 94%, 0.351 g). ^1H NMR (400 MHz, δ ppm) ($\text{DMSO}-d_6$): 7.40–7.44 (m, 2H), 8.01–8.05 (m, 4H), 8.30 (s, 2H), 8.75 (s, 2H). LC–MS (ESI): m/z : 375 $[\text{M}+\text{H}]^+$. Anal. Calc. for $\text{C}_{19}\text{H}_{10}\text{N}_4\text{OS}_2$: C, 60.95; H, 2.69; N, 14.96. Found: C, 60.79; H, 2.78; N, 14.58%.

2.1.2.3. 6,7-Di-thiophen-2-yl-1,3-dithia-5,8-diaza-cyclopenta[*b*]naphthalen-2-one (h). (Yield: 92%, 0.353 g). ^1H NMR (400 MHz, δ ppm) ($\text{DMSO}-d_6$): 7.11–7.14 (m, 2H), 7.26–7.27 (m, 2H), 7.83–7.84 (d, 2H), 8.57 (s, 2H). LC–MS (ESI): m/z : 385 $[\text{M}+\text{H}]^+$. Anal. Calc. for $\text{C}_{17}\text{H}_8\text{N}_2\text{OS}_4$: C, 53.10; H, 2.10; N, 7.29. Found: C, 53.42; H, 2.17; N, 7.68%.



Scheme 3. Synthetic route for compounds a–e and f–j.



$x = 2$, R = pyridin-2-yl (1), pyridin-3-yl (2), thiophen-2-yl (3), furan-2-yl (4)

$x = 1$, R = naphthalen-2-yl (5)

Scheme 4. Synthetic route for new nickel dithiolene complexes.

2.1.2.4. 6,7-Di-furan-2-yl-1,3-dithia-5,8-diaza-cyclopenta[*b*]naphthalen-2-one (**i**). (Yield: 91%, 0.320 g). $^1\text{H NMR}$ (400 MHz, δ ppm) (DMSO- d_6): 6.72–6.79 (m, 4H), 7.92 (s, 2H), 8.58 (s, 2H). LC–MS (ESI): m/z : 353 [M+H] $^+$. Anal. Calc. for $\text{C}_{17}\text{H}_8\text{N}_2\text{O}_3\text{S}_2$: C, 57.94; H, 2.29; N, 7.95. Found: C, 58.26; H, 2.37; N, 8.38%.

2.1.2.5. 6,7-Di-naphthalen-2-yl-1,3-dithia-5,8-diaza-cyclopenta[*b*]naphthalen-2-one (**j**). (Yield: 91%, 0.429 g). $^1\text{H NMR}$ (400 MHz, δ ppm) (DMSO- d_6): 7.45–7.57 (m, 6H), 7.86–7.88 (m, 6H), 8.16–8.22 (m, 3H), 8.76 (s, 1H). LC–MS (ESI): m/z : 473 [M+H] $^+$. Anal. Calc. for $\text{C}_{29}\text{H}_{16}\text{N}_2\text{O}_2\text{S}_2$: C, 73.70; H, 3.41; N, 5.93. Found: C, 74.03; H, 3.45; N, 6.42%.

2.1.3. General procedure for the synthesis of nickel dithiolene coordination complexes 1–5

Sodium metal (30 mg) was added to the 10 mL methanol solution of **f–g** (2 mmol); after getting clear solution, $\text{NiCl}_2 \cdot 6\text{H}_2\text{O}$ (1 mmol) was added and it was stirred for 10 min, followed by the addition of $[\text{PPh}_4]\text{Br}$ (2 mmol). The stirring was continued for an additional 15 min by the addition of 10 mL water, whereby the product was obtained as precipitate, which was filtered and air dried (Scheme 4). The crystals of compounds **2** and **3**, suitable for single crystal X-ray structure determination, were obtained by crystallizing the above mentioned precipitates of **2** and **3** by

the diffusion of diethyl ether to their acetonitrile–methanol solution and acetonitrile solution respectively. Compounds **1**, **4** and **5** were crystallized also by diffusion of diethyl ether to the respective acetonitrile solutions, but we could not obtain crystals, suitable for single crystal X-ray crystallography because of their tiny sizes. The characterization data for compounds **1–5** are described below. Compounds **2** and **3** are additionally characterized by single crystal X-ray crystallography.

2.1.3.1. Compound 1. Yield: 0.124 g (62% based on nickel metal). HRMS: calc: 750.0047, found: 750.0047 (m/z). Anal. Calc. for $\text{C}_{84}\text{H}_{60}\text{N}_8\text{NiP}_2\text{S}_4$: C, 70.54; H, 4.22; N, 7.83%. Found: C, 70.41; H, 4.18; N, 7.96%. IR (KBr, ν/cm^{-1}): 3468, 3051, 2922, 2852, 1635, 1585, 1473, 1431, 1348, 1207, 1087, 995, 860. $^1\text{H NMR}$ (400 MHz, δ ppm) (CD_3CN): 8.12–2.11 (m, 1H), 8.04–7.89 (m, 13H), 7.77–7.65 (m, 40H), 7.62–7.60 (m, 3H), 7.47–7.42 (m, 3H).

2.1.3.2. Compound 2. Yield: 0.103 g (58% based on nickel metal). HRMS: calc. 750.0047, found: 750.0047 (m/z). Anal. Calc. for $\text{C}_{84}\text{H}_{60}\text{N}_8\text{NiP}_2\text{S}_4$: C, 70.54; H, 4.22; N, 7.83%. Found: C, 70.65; H, 4.32; N, 7.79%. IR (KBr, ν/cm^{-1}): 3435, 3049, 2922, 2851, 1583, 1481, 1327, 1205, 1078, 997, 850. $^1\text{H NMR}$ (500 MHz, δ ppm) (CD_3CN): 8.06–8.03 (m, 12H), 7.89–7.85 (m, 21H), 7.83–7.78 (m, 23H), 7.72 (s, 4H).

Table 1
Crystal data and structural refinement for compounds **2** and **3**.

	2	3
Empirical formula	$\text{C}_{80}\text{H}_{60}\text{NiN}_8\text{S}_4\text{P}_2$	$\text{C}_{80}\text{H}_{56}\text{N}_4\text{NiP}_2\text{S}_8$
Formula weight	1430.29	1450.42
T (K)	298	100
Crystal size (mm)	$0.24 \times 0.22 \times 0.18$	$0.28 \times 0.26 \times 0.22$
Crystal system	monoclinic	triclinic
Space group	$P2(1)/c$	$P1$
Z	2	1
λ (Å)	0.71073	0.71073
a (Å)	15.506(5)	9.364(10)
b (Å)	15.916(5)	10.592(11)
c (Å)	15.090(4)	17.983(19)
α (°)	90.00	78.44(2)
β (°)	90.97(2)	76.54(2)
γ (°)	90.00	73.63(2)
V (Å 3)	3723.95(19)	1647.0(3)
D_{calc} (Mg/m 3)	1.276	1.462
Reflections collected/unique	14890/6451	15756/5783
R_{int}	0.0357	0.0485
$F(000)$	1484	750
Maximum and minimum transmission	0.9208 and 0.8964	0.8705 and 0.8393
θ (°)	2.70–25.00	2.03–25.00
Data/restraints/parameters	6451/0/448	5783/0/430
Goodness-of-fit (GOF) on F^2	0.821	1.208
R_1/wR_2 [$I > 2\sigma(I)$]	0.0550/0.1484	0.0704/0.1401
R_1/wR_2 (all data)	0.0911/0.1761	0.0858/0.1464
Largest diff. peak and hole (e Å $^{-3}$)	0.330 and -0.247	0.962 and -0.474

Table 2
Bond lengths (Å) and angles (°) for the compounds **2** and **3**.

Compound 2			
Ni(1)–S(2)	2.1668(9)	S(2)–Ni(1)–S(1)	91.55(3)
Ni(1)–S(1)	2.1798(9)	C(2)–S(2)–Ni(1)	105.29(12)
S(2)–C(2)	1.742(4)	C(31)–P(1)–C(37)	109.6(2)
N(2)–C(8)	1.333(4)	C(31)–P(1)–C(25)	109.2(2)
C(1)–S(1)	1.740(4)	C(1)–S(1)–Ni(1)	104.84(11)
Compound 3			
Ni(1)–S(2)	2.1550(11)	S(2)–Ni(1)–S(1)	91.12(4)
Ni(1)–S(1)	2.1719(11)	C(1)–S(1)–Ni(1)	104.85(15)
S(2)–C(2)	1.726(4)	C(2)–S(2)–Ni(1)	105.63(16)
S(4)–C(16)	1.707(5)	C(7)–N(1)–C(5)	118.3(4)

Table 3
Hydrogen bonding parameters for compounds **2** and **3** (Å and °).

D–H...A	d(D–H)	d(H...A)	d(D...A)	<(DHA)
Compound 2				
C(10)–H(10)···N(3)#1	0.93	2.52	3.363(6)	150.2
C(39)–H(39)···N(3)#2	0.93	2.92	3.653(7)	136.5
Compound 3				
C(31)–H(31)···N(1)#3	0.93	2.85	3.529(6)	131.1
C(22)–H(22)···N(2)#2	0.93	2.85	3.656(6)	145.9
C(27)–H(27)···N(1)#2	0.93	2.86	3.699(6)	151.3
C(11)–H(11)···S(4)#4	0.93	3.02	3.862(5)	151.0

Symmetry transformations used to generate equivalent atoms:

#1 $-x, y + 0.5, -z + 0.5$ #2 $-x, -y + 1, -z + 1$ #3 $-x + 1, -y, -z + 1$ #4 $-x, -y, -z + 1$.

2.1.3.3. Compound 3. Yield: 0.135 g (68% based on nickel metal). HRMS: calc: 770.8572, found: 769.8494 $[M-H]^+$. Anal. Calc. for $C_{80}H_{56}N_4NiP_2S_8$: C, 66.24; H, 3.89; N, 3.86%. Found: C, 66.42; H, 3.96; N, 4.19%. IR (KBr, ν/cm^{-1}): 3437, 2922, 2851, 1641, 1581, 1514, 1483, 1431, 1358, 1203, 1080, 995, 848. 1H NMR

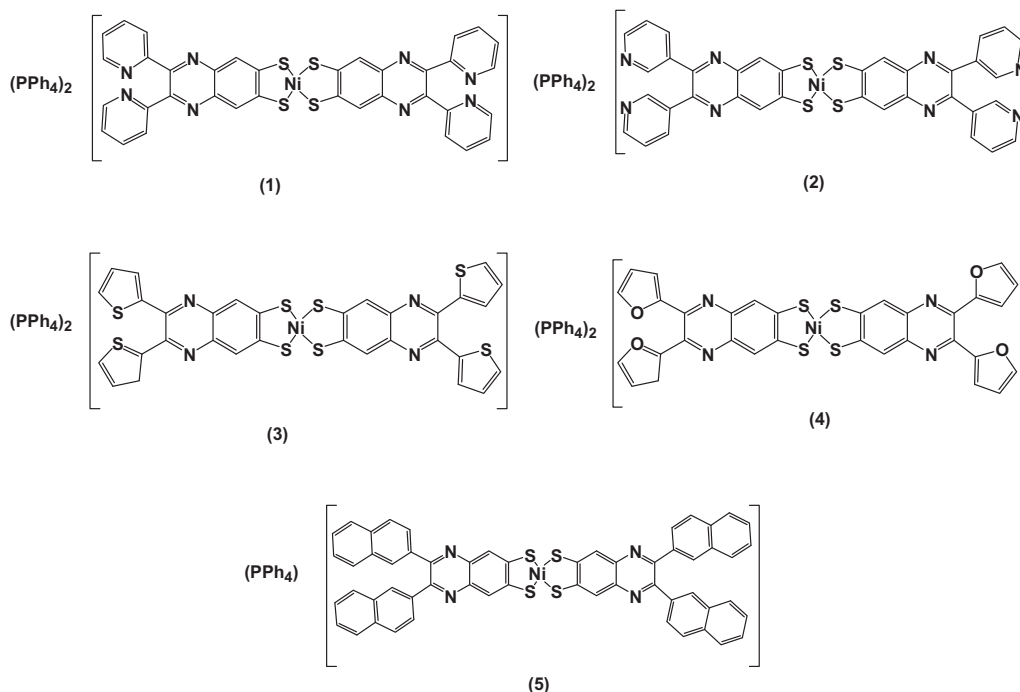
(500 MHz, δ ppm) (CD_3CN): 8.06–8.01 (m, 15H), 7.86–7.54 (m, 33H), 7.43–7.21 (m, 3H), 7.16–7.13 (m, 5H).

2.1.3.4. Compound 4. Yield: 0.122 g (58% based on nickel metal). HRMS: calc: 706.9486, found: 705.9408 $[M-H]^+$. Anal. Calc. for $C_{80}H_{56}N_4NiO_4P_2S_4$: C, 69.31; H, 4.07; N, 4.04%. Found: C, 69.55; H, 4.13; N, 4.49%. IR (KBr, ν/cm^{-1}): 3416, 2922, 2851, 1581, 1481, 1425, 1327, 1251, 1205, 1157, 1078, 997, 887. 1H NMR (400 MHz, δ ppm) (CD_3CN): 7.93–7.86 (m, 5H), 7.77–7.70 (m, 15H), 7.69–7.65 (m, 7H), 7.63–7.60 (m, 5H), 7.47–7.42 (m, 14H), 7.26–7.22 (m, 8H), 7.17–7.15 (m, 2H).

2.1.3.5. Compound 5. Yield: 0.128 g (57% based on nickel metal). HRMS: calc: 946.0863, found: 946.0863 (m/z). Anal. Calc. for $C_{80}H_{52}N_4NiPS_4$: C, 74.65; H, 4.07; N, 4.35%. Found: C, 74.52; H, 4.12; N, 4.43%. IR (KBr, ν/cm^{-1}): 3439, 3053, 2962, 2924, 2852, 1658, 1624, 1593, 1433, 1352, 1261, 1176, 1082, 906, 860. 1H NMR (500 MHz, δ ppm) (CD_3CN): 8.24–8.22 (m, 6H), 8.17–8.13 (m, 7H), 8.09–8.08 (m, 2H), 8.05–8.02 (m, 5H), 7.88–7.84 (m, 12H), 7.82–7.78 (m, 10H), 7.75–7.70 (m, 5H), 7.67–7.60 (m, 5H).

2.2. Crystal structure determination

Crystal data of compound **2** were measured at 298(2) K on Oxford Gemini Diffractometer equipped with EOS CCD detector. Monochromatic Mo $K\alpha$ radiation ($\lambda = 0.71073$ Å) was used for the measurements. Absorption corrections using multi ψ -scans were applied. Single crystals, suitable for facile structural determination for the compound **3**, was measured at 100(2) K on a three circle Bruker SMART APEX CCD area detector system under Mo $K\alpha$ ($\lambda = 0.71073$ Å) graphite monochromatic X-ray beam, 2400 frames were recorded with an ω scan width of 0.3°, each for 10 s, crystal-detector distance 60 mm, collimator 0.5 mm. Data reduction was performed by using SAINTPLUS [27]. Empirical absorption corrections were performed by using equivalent reflections performed program SADABS [27]. The structures were solved by direct methods

**Scheme 5.** Structural representation of synthesized nickel dithiolenes complexes **1–5**.

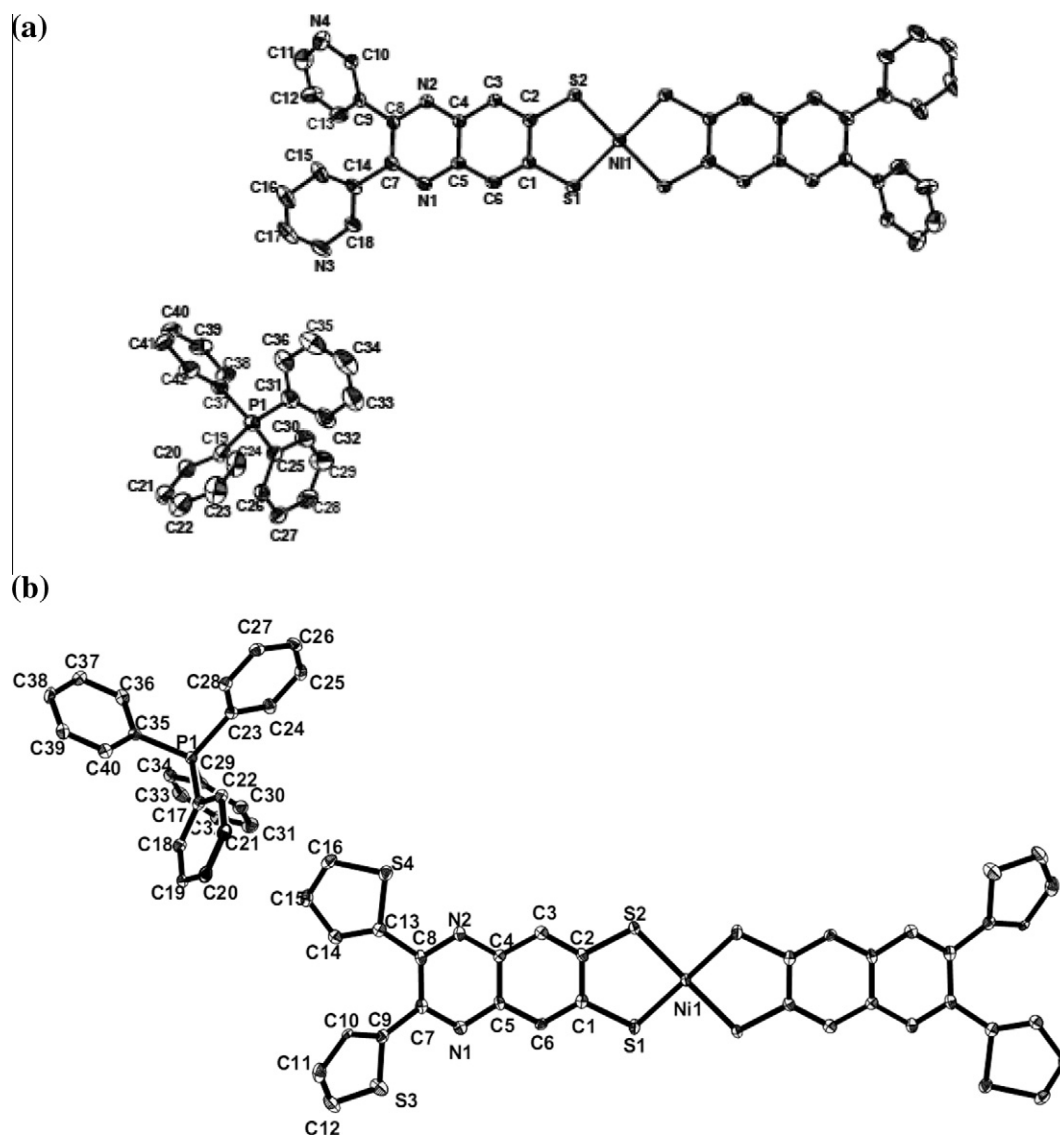


Fig. 1. Thermal ellipsoidal diagrams of (a) compound **2** (20% probability), (b) compound **3** (40% probability, hydrogen atoms are omitted for clarity).

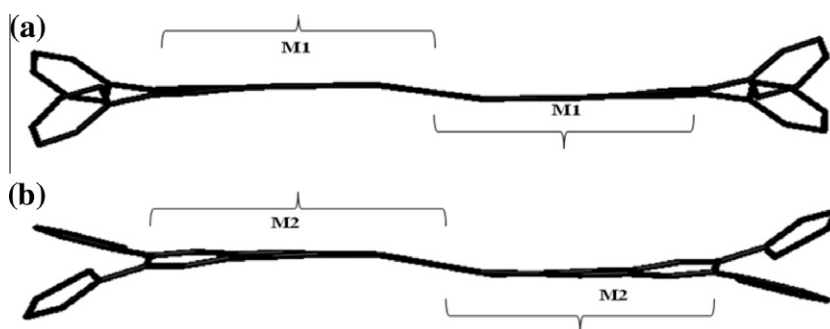


Fig. 2. (a) Mean plane (M1) of the half dithiolene unit (Ni1S1C1C6C5N1C7C8N2C4C3C2S2) in compound **2** and (b) mean plane (M2) of the half dithiolene unit (Ni1S1C1C6C5N1C7C8N2C4C3C2S2) in compound **3**.

and least-square refinement on F^2 for the compounds **2** and **3** by using SHELXS-97 [28]. All non-hydrogen atoms were refined

anisotropically. The hydrogen atoms were included in the structure factor calculation by using a riding model. The crystallographic

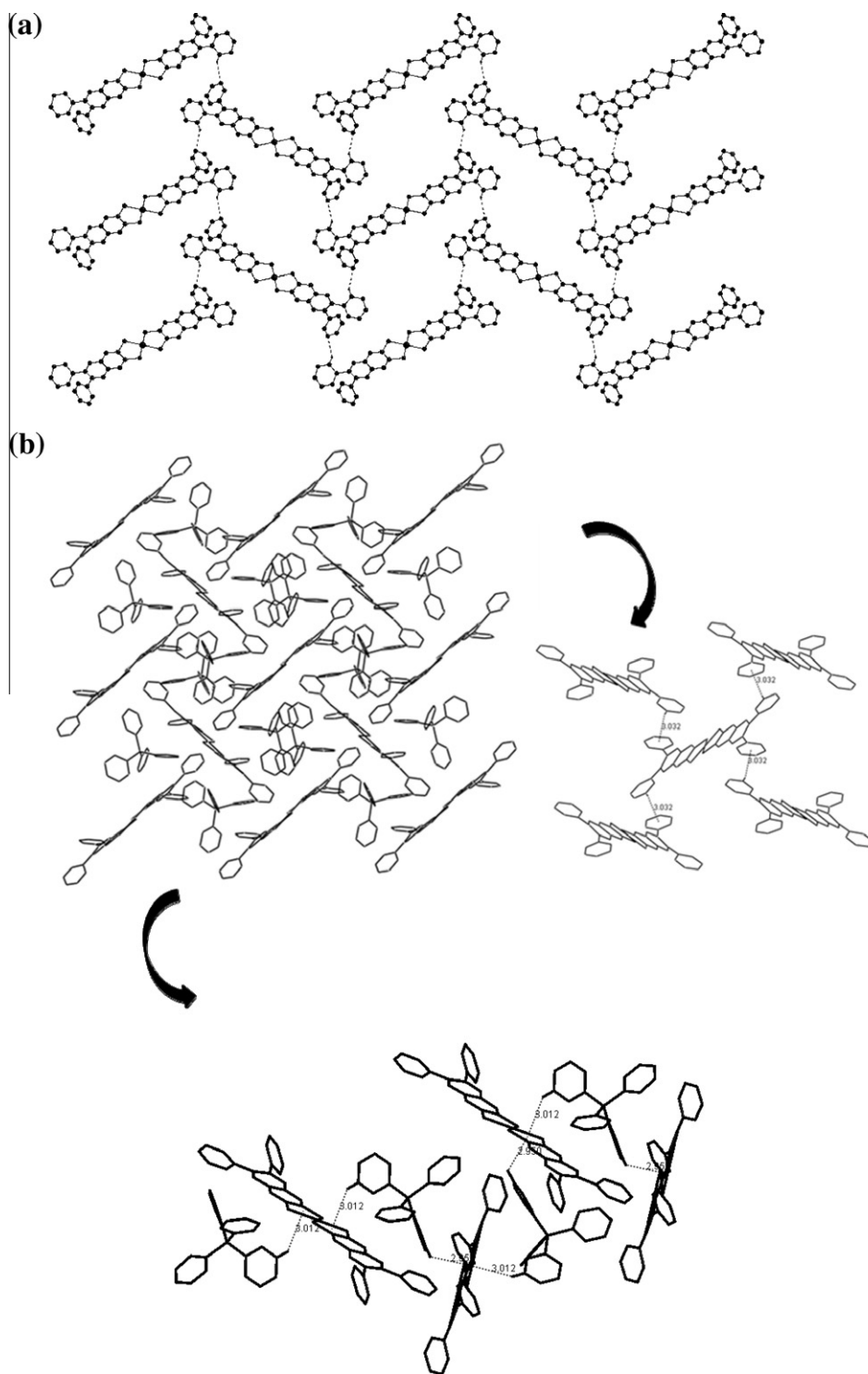


Fig. 3. (a) Molecular packing diagram of the compound **2** characterized by C–H...N weak interactions resulting in two dimensional supramolecular layer, (b) C–H... π interactions between pyridyl rings from the anion moiety and C–H... π interactions between centroid of the metal chelate ring and cation (tetraphenylphosphonium), (c) Two-dimensional supramolecular network through C–H...N hydrogen bonding interactions in the crystal structure of compound **3**.

parameters, data collection and structure refinement of the compounds **2–3** are summarized in Table 1. Selected bond lengths and bond angles for the compounds **2** and **3** are listed in Table 2. The supramolecular hydrogen bonding interactions in the crystal

structures of compounds **2** and **3** are presented in Table 3. In the crystal structure of complex **2**, the disordered solvent contributions were removed by the SQUEEZE [29] command in the PLATON program.

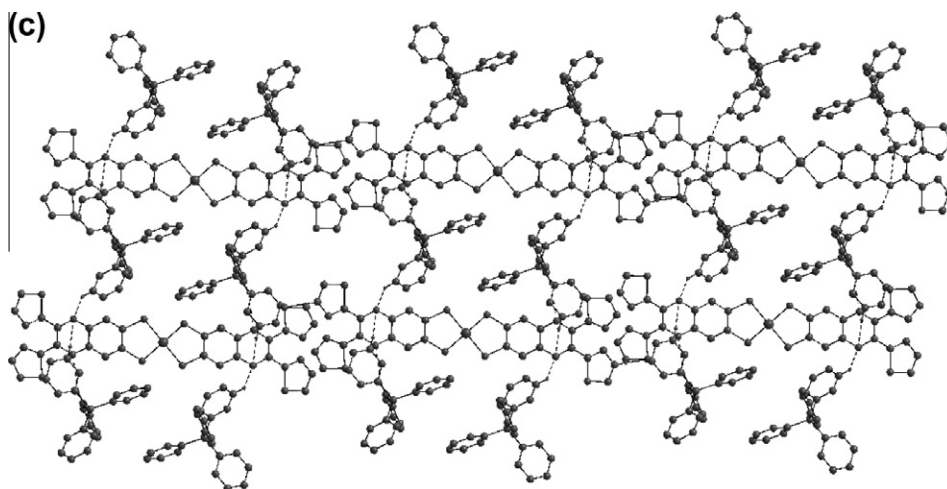


Fig. 3. (continued)

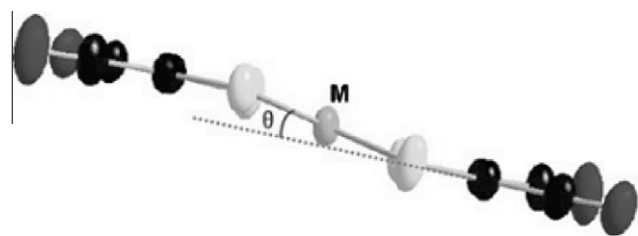


Fig. 4. Z-shaped nonplanar geometry.

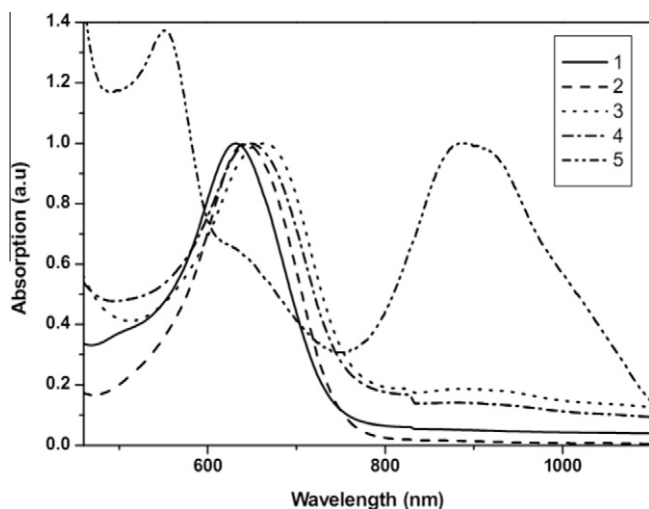


Fig. 5. Normalised electronic absorption spectra for compounds 1–5 in acetonitrile solution.

3. Results and discussion

3.1. Synthesis

Compounds **1–5** have been synthesized by the reaction of one equivalent $\text{NiCl}_2 \cdot 6\text{H}_2\text{O}$ with two equivalents of di-substituted-1,3-dithia-5,8-diaza-cyclopenta[*b*]naphthalen-2-ones (**f–j**) in MeOH treated with sodium metal at an ambient condition and then precipitated by adding tetraphenylphosphonium bromide, yielding the microcrystalline form of compounds **1–5** in reasonable

yield. Diagrammatic representations of the compounds **1–5** have been shown in Scheme 5.

3.2. Molecular and crystal structures

The block-shaped-crystals of compound $(\text{PPh}_4)_2[\text{Ni}(\text{C}_{18}\text{H}_{10}\text{N}_4\text{S}_2)_2]$ (**2**) were crystallized in monoclinic space group $P(2)/c$, whereas compound $(\text{PPh}_4)_2[\text{Ni}(\text{C}_{16}\text{H}_8\text{N}_2\text{S}_4)_2]$ (**3**) was crystallized in triclinic space group $P\bar{1}$. The asymmetric units in the crystal structures of compounds **2** and **3** (represented as labeled atoms in Fig. 1) contain half molecule of nickel–dithiolene moiety and one tetraphenylphosphonium cation. The average Ni–S bond distances in the crystal structure of compound **2** is 2.173 Å, whereas in compound **3**, it is 2.163 Å. The distance between two mean planes of chelate rings Ni1S1C1C2S2 in $[\text{Ni}(\text{C}_{18}\text{H}_{10}\text{N}_4\text{S}_2)_2]^{2-}$ (**2**) and $[\text{Ni}(\text{C}_{16}\text{H}_8\text{N}_2\text{S}_4)_2]^{2-}$ (**3**) are 0.149 Å and 0.172 Å respectively. The dihedral angle between two S1NiS2 planes in both the compounds **2** and **3** is 0° , that is, the $c_1\text{–Ni–}c_2$ angle is 180° (c_1 and c_2 are the midpoints of the sulfur atoms in the five-membered chelate rings), which indicates the geometry around nickel metal centre is perfectly square planar in both compounds. The angle between two pyridin-3-yl rings (C14C15C16C17N3C18 and C9C10N4C11C12C13) in compound **2** is 62.20° , and angle between two thiophen-2-yl rings (C9C10C11C12S3 and C13S4C14C15C16) is 51.96° in compound **3**. This indicates that, due to the large size of the pyridin-3-yl rings (steric effect), the concerned angle is larger in compound **2** compared to that in compound **3**. The bending angles (η) between {S1NiS2} and {S1C1C2S2} planes present in the {Ni1S1C1C2S2} dithiolate-chelated ring are 9.78° and 11.31° in compounds **2** and **3** respectively. The distance between two mean planes in compound **2** is 0.423 Å (M1 in Fig. 2), whereas in compound **3** this distance (M2) between two mean planes is 0.526 Å. As shown in Fig. 2, the half moiety of M1, which is present in compound **2**, is more planar than the half moiety of M2 which is present in compound **3**.

The weak interactions between pyridine moieties with a distance 2.52 Å ($\text{H}\cdots\text{A}$) of C(10)–H \cdots N(3) hydrogen bond in compound **2** lead to a two dimensional supramolecular network (Fig. 3a). In the crystal structure of compound **2**, there are additional C(16)–H \cdots π (H16 \cdots Cg, Cg = C9C10C11C12C13N4) interactions between pyridine moieties with a distance of 3.032 Å; these interactions involve four anionic moieties around one anionic moiety, as shown in Fig. 3(b). In addition to this, there are other C–H \cdots π interactions C–H(29) \cdots Cg and C–H(34) \cdots Cg ($\text{H}\cdots\text{Cg}$ = 3.012 and 2.950 Å respectively), that are present between phenyl moiety

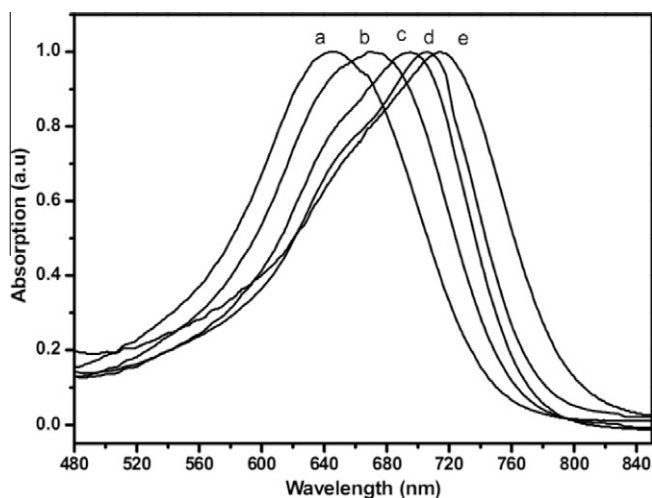


Fig. 6. Absorption spectra of compound **2** in different solvents at room temperature, (a) acetonitrile, (b) DMSO, (c) DMF, (d) acetone, (e) chloroform.

(from tetraphenylphosphonium cation) and the centroid (Cg) of the NiS1C1C2S2 chelate ring system. Compound **3** also offers a 2-D network through C–H···N supramolecular interactions as shown in Fig. 3(c). A prominent feature of the structural aspect for these two complexes is that $[\text{Ni}(\text{C}_8\text{H}_2\text{N}_2\text{S}_2\text{R}_2)_2]^{2-}$ (R = pyridin-3-yl and thiophen-2-yl) exhibit non-planar Z-shaped geometry with the ligand fragments, that are bent away from the {NiS4} planes with a dihedral angle of 11.14° in compound **2** and 14.28° in compound **3** (Fig. 4); these values are comparable to those of known copper dithiolene complexes [30].

3.3. UV–Vis absorption spectra for compounds 1–5

Fig. 5 shows the electronic absorption spectra of the complexes **1–5** in acetonitrile. The absorption maxima of the compounds **1–5** are observed at 635, 639, 665, 649 and 892 nm respectively. These absorption bands can be attributed to the charge transfer transitions (CT) involving electronic excitation from a HOMO which is a mixture of dithiolate (π) and metal (d) orbital character to a LUMO which is a π^* orbital of the dithiolate [31,32]. The extent of the relative shift in the absorption maximum of each complex is explained based on the extent of delocalization (in the chelate ring) induced by the substituent. The absorption spectra of complexes **1** and **2** did not deviate much from one another and the close proximity of their maxima is due to the identical nature of the pyridin-2-yl and pyridin-3-yl substituents, present in compounds **1** and **2** respectively. However, it is noticed that simple exchange of furan-2-yl (compound **4**) by thiophen-2-yl (compound **3**) enhances the extent of electron delocalization (in compound **3**), which is responsible for the red shift of the absorption maximum of complex **3** (665 nm) compared to that of complex **4** (649 nm). Putting more π -electron cloud by introducing naphthalene substituent in complex **5** drastically shifts the absorption maximum of the complex into the near IR region with absorption maximum at 892 nm. The influence of different substituents with different electron delocalization capabilities on the spectral properties of the nickel complexes is known in literature and the results observed in the present study are in accord with the mechanisms explained (in literature) that are based on the delocalization effects of the substituents [15,33].

Interestingly, complexes **1** and **2**, in the present work, show negative solvatochromic behavior with a blue shift in the spectral maximum with increase in solvent polarity. Fig. 6 represents the negative solvatochromic behavior of complex **2** with a change in

the absorption maximum from 714 nm in chloroform to 639 nm in acetonitrile. This solvatochromic behavior of compounds **1** and **2** indicates more charge transfer nature of the ground state than the excited state [34–36]. Increase in polarity of the solvent stabilizes the ground state more than the excited state, which further increases the energy gap between the HOMOs and LUMOs in dithiolene complexes (for example, in the present study, complexes **1** and **2**). The increase in this energy gap with increase in solvent polarity results in blue shift of the observed absorption maximum. Unlike compounds **1** and **2**, complexes **3–5** did not show any solvatochromic behavior.

3.4. Electrochemistry

The electrochemical behavior of the complexes **1–5** were performed in dimethylsulfoxide solution, which contained $[\text{Bu}_4\text{N}][\text{ClO}_4]$ (TBAP) as supporting electrolyte and platinum as working electrode. We have characterized compounds **1–4** as Ni(II) coordination complexes and compound **5** as Ni(III) complex. Compound **1** exhibits a reversible oxidative response at $E_{1/2} = 0.17$ V ($\Delta E = 92$ mV) versus Ag/AgCl (under identical condition, Fc^+/Fc couple is observed at 0.53 V, see in the section of Supplementary materials). Compound **2** shows a reversible oxidative response at $E_{1/2} = +0.21$ V ($\Delta E = 83$ mV) versus Ag/AgCl. Compounds **3** and **4** exhibit quasi-reversible oxidative responses at $E_{1/2} = 0.18$ V

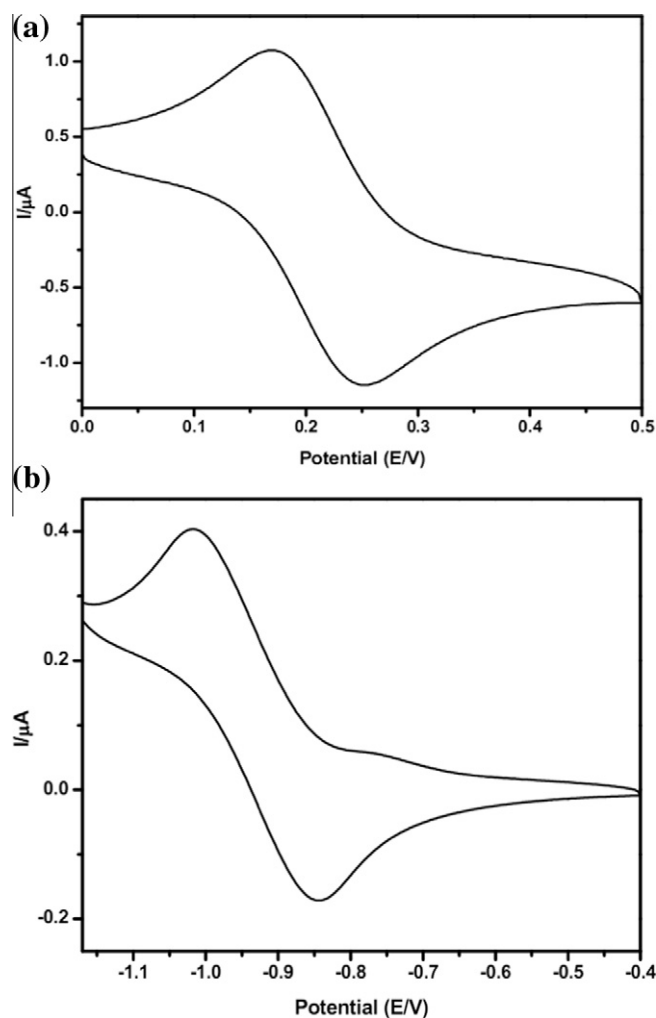


Fig. 7. (a) Cyclic voltammogram of compound **2** in TBAP/DMSO at scan rate 50 mVs^{-1} . (b) Cyclic voltammogram (reductive response) of the complex **5**.

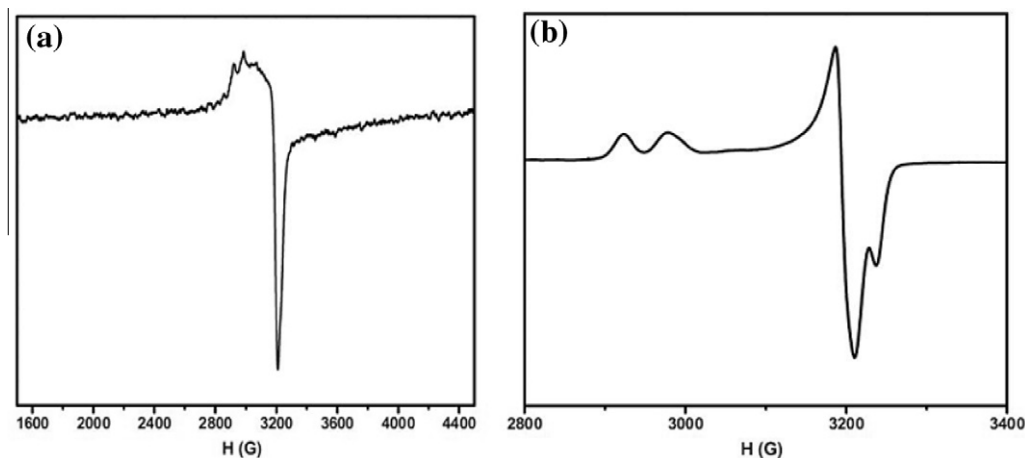


Fig. 8. EPR spectra of the compound **5**: (a) powder form at room temperature, (b) frozen state (in DMF) at liquid nitrogen temperature.

($\Delta E = 120$ mV) and 0.17 V ($\Delta E = 132$ mV) versus Ag/AgCl respectively. These oxidative responses correspond to the respective $[\text{Ni}^{\text{III}}(\text{C}_8\text{H}_2\text{N}_2\text{S}_2\text{R}_2)_2]^{1-}/[\text{Ni}^{\text{II}}(\text{C}_8\text{H}_2\text{N}_2\text{S}_2\text{R}_2)_2]^{2-}$ redox couples. A representative cyclic voltammogram of compound **2** is shown Fig. 7(a) (see the section of Supplementary data for the CV diagrams of compounds **1**, **3**, **4**). According to literature [37–40], usually Ni(II)-bis(dithiolene) complexes exhibit oxidative responses within the range of $E_{1/2} = +0.12$ to $+0.41$ V. Thus compounds **1–4**, having lower oxidation potential values, can be relatively easily oxidized to their respective Ni(III) species. Compound **5** (a nickel(III) complex) shows a quasi-reversible oxidative response (see the section of Supplementary data for the relevant diagram) at $E_{1/2} = 0.09$ V ($\Delta E = 111$ mV) which corresponds the $[\text{Ni}^{\text{IV}}(\text{C}_8\text{H}_2\text{N}_2\text{S}_2\text{R}_2)_2]^0/[\text{Ni}^{\text{III}}(\text{C}_8\text{H}_2\text{N}_2\text{S}_2\text{R}_2)_2]^{1-}$ ($\text{R} = \text{naphthalen-2-yl}$). The very low oxidation potential of compound **5** indicates that this compound is very susceptible to oxidation to corresponding Ni(IV) complex. Probably the electron drift from metal center to the substituent naphthalene ring by resonance effect is responsible for this low oxidation potential of compound **5**. For the same reason, compound **5** would be difficult to reduce to its corresponding Ni(II) species. Thus, compound **5** exhibits a quasi reversible reductive response at $E_{1/2} = -0.93$ V ($\Delta E = 173$ mV) versus Ag/AgCl, which corresponds to the $[\text{Ni}(\text{C}_8\text{H}_2\text{N}_2\text{S}_2\text{R}_2)_2]^{1-}/[\text{Ni}(\text{C}_8\text{H}_2\text{N}_2\text{S}_2\text{R}_2)_2]^{2-}$ redox couple (Fig. 7(b)). It is worth mentioning that compounds **3** and **4** have the similar oxidation potentials indicating that both these compounds have identical stabilities towards the chemical oxidation. Based on the literature [41–43], thiophene-containing nickel dithiolene complexes are more favorable towards electropolymerization. In the present study, compound **3** (a thiophene-containing nickel dithiolene complex) can be easily oxidized (considering its oxidation potential value) to a neutral species $[\text{Ni}(\text{C}_8\text{H}_2\text{N}_2\text{S}_2\text{R}_2)_2]$ ($\text{R} = \text{thiophen-2-yl}$), which might not be suitable for the electropolymerization.

3.5. ESR spectroscopy

The electrochemical studies of compound **5**, suggesting that it should be Ni(III) complex at its resting state, prompted us to perform ESR studies of compound **5**. The ESR spectra of solid samples of compound **5** were recorded at room temperature and at liquid nitrogen temperature; room temperature solution state ESR spectrum of compound **5** has also been recorded (see Section-8 in Supplementary data). Compound **5** exhibits a rhombic type signal ($g_x = 2.237$, $g_y = 2.195$ and $g_z = 2.044$) at liquid nitrogen temperature as shown in Fig. 8. The ESR studies indicate that compound **5** is a Ni(III) complex. Based on the literature [44–46], the g_{av} values are in the range of 2.12–2.16 for a d^7 low-spin electron config-

uration, probable for a 3+ formal oxidation state of nickel. The g_{av} value of the compound **5** is 2.158, which implies that nickel metal in this compound has the 3+ oxidation state. The anisotropy in the ESR spectra implies some contribution of the d-orbitals of nickel in the total spin density, which is usually, in this class of compounds [47,48], distributed 40% on nickel and 60% on the ligands.

4. Conclusion

We have described here *N*-heterocyclic based nickel-bis(dithiolene) complexes $(\text{PPh}_4)_2[\text{Ni}(\text{C}_8\text{H}_2\text{N}_2\text{S}_2\text{R}_2)_2]$ ($\text{R} = \text{pyridin-2-yl}$ (**1**), pyridin-3-yl (**2**), thiophen-2-yl (**3**), furan-2-yl (**4**)) and $(\text{PPh}_4)[\text{Ni}(\text{C}_8\text{H}_2\text{N}_2\text{S}_2\text{R}_2)_2]$ ($\text{R} = \text{naphthalen-2-yl}$ (**5**)). Complexes **2** and **3** have been characterized by X-ray crystallography; the relevant analysis shows supramolecular weak interactions in the crystal structures and the distortion in square-planar geometry around the metal ion in terms of dihedral angle (λ) between two SMS planes and bending angle (η) (between the SMS and SCCS planes) of dithiolene chelate ring system. We have compared the effect of dithiolene-substituents on the electronic absorption spectral shift. Charge transfer absorption bands in compounds **1** and **2** (635 and 639 nm) are influenced by the solvent polarity, and hence it shows a negative solvatochromism (absorption band is shifted towards blue shift for the more polar solvent). An important aspect of the present study is that compound **5** (a Ni(III) complex) is oxidized electrochemically at a very low oxidation potential meaning that complex $(\text{PPh}_4)[\text{Ni}^{\text{III}}(\text{C}_8\text{H}_2\text{N}_2\text{S}_2\text{R}_2)_2]$ (**5**) ($\text{R} = \text{naphthalen-2-yl}$) would be easily oxidized to its corresponding Ni(IV) compound $[\text{Ni}^{\text{IV}}(\text{C}_8\text{H}_2\text{N}_2\text{S}_2\text{R}_2)_2]$. The isolation and further studies of such Ni(IV) complexes are in progress in our laboratory.

Acknowledgements

We thank Department of Science and Technology, Government of India, for financial support (Project No. SR/SI/IC-23/2007). The National X-ray Diffractometer facility at University of Hyderabad by the Department of Science and Technology, Government of India, is gratefully acknowledged. We are grateful to UGC, New Delhi, for providing infrastructure facility at University of Hyderabad under UPE grant. RK thanks CSIR, New Delhi, for their fellowship. We thank to Mr. K. Santhosh, Mr. Suresh (EPR) for helpful discussion in preparing this manuscript. We are grateful to Professor S. Pal and his co-workers for providing us the facility of electrochemical experiments.

Appendix A. Supplementary material

CCDC 893972 and 893973 contain the supplementary crystallographic data for this paper. These data can be obtained free of charge via <http://www.ccdc.cam.ac.uk/conts/retrieving.html>, or from the Cambridge Crystallographic Data Centre, 12 Union Road, Cambridge CB2 1EZ, UK; fax: +44 1223 336 033; or e-mail: deposit@ccdc.cam.ac.uk. Supplementary data associated with this article can be found, in the online version, at <http://dx.doi.org/10.1016/j.poly.2012.11.046>.

References

- [1] R.P. Burns, C.A. McAuliffe, *Adv. Inorg. Chem. Radiochem.* 22 (1979) 303.
- [2] N. Robertson, L. Cronin, *Coord. Chem. Rev.* 227 (2002) 93.
- [3] J.A. McCleverty, *Prog. Inorg. Chem.* 10 (1969) 49.
- [4] R. Eisenberg, *Prog. Inorg. Chem.* 12 (1970) 295.
- [5] U.T. Mueller-Westerhoff, B. Vance, in: G. Wilkinson, R.D. Gillard, J.A. McCleverty (Eds.), *Comprehensive Coordination Chemistry*, vol. 2, Pergamon, Oxford, 1987. Chapter 16.5.
- [6] A.E. Pullen, C. Faulmann, K.I. Pokhodnya, P. Cassous, M. Tokumoto, *Inorg. Chem.* 37 (1998) 6714.
- [7] A. Davison, N. Edelstein, R.H. Holm, A.H. Maki, *J. Am. Chem. Soc.* 85 (1963) 2029.
- [8] H. Adams, A.M. Coffey, M.J. Morris, S.A. Morris, *Inorg. Chem.* 48 (2009) 11945.
- [9] M.D. Ward, J.A. McCleverty, *J. Chem. Soc., Dalton Trans.* (2002) 275.
- [10] H. Tanaka, Y. Okano, H. Kobayashi, W. Suzuki, A. Kobayashi, *Science* 291 (2001) 285.
- [11] S.N. Oliver, S.V. Kershaw, A.E. Underhill, C.A.S. Hill, A. Charlton, *MCLC S&T Sect. B* 10 (1995) 87.
- [12] K. Wang, E.I. Stiefel, *Science* 291 (2001) 106.
- [13] M. Fourmigue, *Acc. Chem. Res.* 37 (2004) 179.
- [14] U.T. Mueller-Westerhoff, B. Vance, D.I. Yoon, *Tetrahedron* 47 (1991) 909.
- [15] P. Basu, A. Nigam, B. Mogesa, S. Denti, V.N. Nemykin, *Inorg. Chim. Acta* 363 (2010) 2857.
- [16] T.-T. Bui, O. Thieubaut, E. Grelet, M.-F. Achard, B.G.-de. Bonneval, K.I.M.-C. Ching, *Eur. J. Inorg. Chem.* (2011) 2663.
- [17] S. Rabaca, A.C. Cerdeira, S. Oliveira, I.C. Santos, R.T. Henriques, L.C.J. Pereira, J.T. Coutinho, M. Almeida, *Polyhedron* 39 (2012) 91.
- [18] H.-J. Lee, D.-Y. Noh, *Polyhedron* 19 (2000) 425.
- [19] S. Rabaca, A.C. Cerdeira, A.I.S. Neves, S.I.G. Dias, C. Mezier, I.C. Santos, L.C.J. Pereira, M. Fourmigue, R.T. Henriques, M. Almeida, *Polyhedron* 28 (2009) 1069.
- [20] Y. Tian-Ming, Z. Jing-Lin, Y. Xiao-Zeng, *Polyhedron* 14 (1995) 1487.
- [21] J.-L. Zuo, T.-M. Yao, F. You, X.-Z. You, H.-K. Fun, B.-C. Yip, *J. Mater. Chem.* 6 (1996) 1633.
- [22] J.L. Brusso, O.P. Clements, R.C. Haddon, M.E. Itkis, A.A. Leitch, R.T. Oakley, R.W. Reed, J.F. Richardson, *J. Am. Chem. Soc.* 126 (2004) 8256.
- [23] C. Jia, S.-X. Liu, C. Tanner, C. Leiggner, A. Neels, L. Sanguinet, E. Levillain, S. Leutwyler, A. Hauser, X. Decurtins, *Chem.-Eur. J.* 13 (2007) 3804.
- [24] E.H. Morkved, T. Andreassen, V. Novakova, P. Zimcik, *Dyes Pigm.* 82 (2009) 276.
- [25] L.E. Harrington, J.F. Britten, D.W. Hughes, A.D. Bain, J.-Y. Thepot, M.J. McGlinchey, *J. Organomet. Chem.* 656 (2002) 243.
- [26] R. Bolligarla, S.K. Das, *Tetrahedron Lett.* 52 (2011) 2496.
- [27] Bruker, SADABS, SMART, SAINT and SHELXTL, Bruker AXS Inc., Madison, Wisconsin, USA, 2000.
- [28] G.M. Sheldrick, *Acta Crystallogr., Sect. A* 64 (2008) 112.
- [29] P.V.D. Sluis, A.L. Speak, *Acta Crystallogr., Sect. A* 46 (1990) 194.
- [30] F.-M. Wang, L.-Z. Chen, Y.-M. Liu, C.-S. Lu, X.-Y. Duan, Q.-J. Meng, *J. Coord. Chem.* 65 (2012) 87.
- [31] S.D. Cummings, R. Eisenberg, *Inorg. Chem.* 34 (1995) 2007.
- [32] S.I. Shupack, E. Billig, R.J.H. Clark, R. Williams, H.B. Gray, *J. Am. Chem. Soc.* 86 (1964) 4594.
- [33] H. Horie, A. Takagi, H. Hasebe, T. Ozawa, K. Ohta, *J. Mater. Chem.* 11 (2001) 1063.
- [34] C. Reichardt, *Chem. Rev.* 94 (1994) 2319.
- [35] C. Reichardt, *Chem. Soc. Rev.* 21 (1992) 147.
- [36] S. Cha, M.G. Choi, H.R. Jeon, S.-K. Chang, *Sens. Actuators, B* 157 (2011) 14.
- [37] R. Bolligarla, S.K. Das, *Eur. J. Inorg. Chem.* (2012) 2933.
- [38] R. Bolligarla, G. Durgaprasad, S.K. Das, *Inorg. Chem. Commun.* 14 (2011) 809.
- [39] R. Bolligarla, G. Durgaprasad, S.K. Das, *Inorg. Chem. Commun.* 12 (2009) 355.
- [40] R. Bolligarla, R. Kishore, G. Durgaprasad, *Inorg. Chim. Acta* 363 (2010) 3061.
- [41] T. Anjos, S.J. Roberts-Bleming, A. Charlton, N. Robertson, A.R. Mount, S.J. Coles, M.B. Hursthouse, M. Kalaji, P.J. Murphy, *J. Mater. Chem.* 18 (2008) 475.
- [42] P.J. Skabara, C. Pozo-Gonzalo, N.L. Miazza, M. Laguna, E. Cerrada, A. Luquin, B. Gonzalez, S.J. Coles, M.B. Hursthouse, R.W. Harrington, W. Clegg, *Dalton Trans.* (2008) 3070.
- [43] C. Pozo-Gonzalo, R. Berridge, P.J. Skabara, E. Cerrada, M. Laguna, S.J. Coles, M.B. Hursthouse, *Chem. Commun.* (2002) 2408.
- [44] B. de Castro, C. Freire, *Inorg. Chem.* 29 (1990) 5113.
- [45] C. Freire, B. de Castro, *Polyhedron* 17 (1998) 4227.
- [46] V. Madhu, S.K. Das, *Inorg. Chem.* 47 (2008) 5055.
- [47] K. Ray, T. Weyhermuller, F. Neese, K. Wieghardt, *Inorg. Chem.* 44 (2005) 5345.
- [48] S. Kokatam, K. Ray, J. Pap, E. Bill, W.E. Geiger, R.J. LeSuer, P.H. Rieger, T. Weyhermuller, F. Neese, K. Wieghardt, *Inorg. Chem.* 46 (2007) 1100.